1-2009

Flexural vibration spectra of carbon nanotubes measured using laser Doppler vibrometry

Laura Biedermann
Purdue University - Main Campus, biedermann@purdue.edu

Ryan C. Tung
Purdue University - Main Campus

Arvind Raman
Birck Nanotechnology Center, Purdue University, raman@purdue.edu

R. Reifenberger
Birck Nanotechnology Center, Purdue University, reifenbr@purdue.edu

Nanotechnology **20** (2009) 035702 (6pp) doi:10.1088/0957-4484/20/3/035702

Flexural vibration spectra of carbon nanotubes measured using laser Doppler vibrometry

Laura B Biedermann[1], Ryan C Tung[2], Arvind Raman[2] and Ronald G Reifenberger[1]

[1] Department of Physics and Birck Nanotechnology Center, Purdue University, W Lafayette, IN 47907, USA
[2] School of Mechanical Engineering and Birck Nanotechnology Center, Purdue University, W Lafayette, IN 47907, USA

Received 7 May 2008, in final form 30 September 2008
Published 17 December 2008
Online at stacks.iop.org/Nano/20/035702

Abstract
Laser Doppler vibrometry is used to measure the thermal vibration spectra of individual multiwalled carbon nanotubes (MWNTs) under ambient conditions. Since the entire vibration spectrum is measured with high frequency resolution, the resonant frequencies and quality factors of the MWNTs are accurately determined, allowing for estimates of their elastic moduli. Because the diameters of the MWNTs studied are smaller than the wavelength of the vibrometer's laser, Mie scattering is used to estimate values for the smallest diameter nanotube or nanowire whose vibration can be measured in this way.

(Some figures in this article are in colour only in the electronic version)

1. Introduction

Vibrating nanomechanical systems are gaining interest for potential applications in ultra-high frequency resonators, sensors, and nanoelectronics, yet few methods exist to reliably measure their motion. A real-time technique capable of measuring the vibration of an individual nanotube or nanowire would enable the design of sensitive chemical sensors and the use of nanotubes and nanowires as oscillators in nanomechanical systems. Of interest are the resonant frequencies of various eigenmodes of oscillation, the quality factor characterizing each resonant eigenmode, and the nanowire material properties required to explain each resonance.

A number of methods to determine the resonant frequency of a carbon nanotube have been published. Electrically excited resonant vibrations of a cantilevered MWNT were observed in a transmission electron microscope (TEM) [1] and from the field emission pattern of a vibrating MWNT [2]. The oscillation of a suspended, doubly clamped MWNT, excited using an oscillating gate voltage, was detected from the modulation in the conductance of the suspended device [3, 4]. The shape of the first three bending eigenmodes of a suspended, doubly clamped MWNT was measured using an atomic force microscope (AFM) [5]. These techniques require either high vacuum conditions or complicated fabrication methods that utilize advanced lithographic techniques. Furthermore, driven methods for measuring resonance can be susceptible to whirling instabilities [6]. For this reason, measuring thermal noise is ideal for resonance frequency measurements. A feature common to all these methods is the low frequency resolution that accompanies the measurement of the MWNT vibration spectrum.

Laser Doppler vibrometry uses the Doppler shift of a reflected laser beam from a vibrating object to measure that object's vibrational velocity; this method has been used to detect the oscillations of microelectromechanical systems (MEMS) devices such as microcantilevers and rotational oscillators [7, 8] as well as silicon nanowires [9]. Laser Doppler vibrometers (LDVs) are well suited for real-time measurements of oscillations up to frequencies of tens of megahertz with high frequency resolution, enabling a precise determination of resonant frequencies and quality factors of the different eigenmodes. However, Doppler vibrometry has scarcely been used to measure the vibration of nanostructures whose dimensions are much smaller than the wavelength and spot size of the laser.

In what follows, we describe the techniques and results obtained using a Polytec MSA-400 scanning LDV to measure and characterize the vibration spectra of a number of thermally excited plasma enhanced chemical vapor deposition (PECVD) grown MWNTs. While this work only discusses measurements of the vibration spectra of MWNTs, the techniques developed are completely general and can be used under ambient or vacuum conditions to measure the vibration spectra of a wide variety of suspended and cantilevered nanotubes and nanowires.

2. Experiment details

The thermal vibration spectra of a MWNT are recorded using a Polytec MSA-400 scanning LDV that is located on a vibration isolation slab[3]. The incident beam of the interferometer (wavelength $\lambda = 633$ nm; power <1 mW) is focused through a 50× microscope objective and is incident normal to the oscillating MWNT. The MWNT's oscillatory motion with amplitude A and velocity v at frequency f caused the backscattered light, which the LDV collects, to be Doppler shifted by a frequency

$$\Delta(t) = \nu' - \nu = -\frac{\mathsf{v}}{c}\nu \cos(2\pi f t), \tag{1}$$

where $\mathsf{v} = \mathsf{A}(2\pi f)$ and $\nu = c/\lambda$, where c is the speed of light. When the Doppler frequency shift is measured at an eigenmode of the MWNT, $\Delta(t)$ is proportional to the resonant frequency f_j and amplitude A_j of the jth eigenmode. The LDV can measure velocities in the spectral range from 0 to 1.5 MHz and displacements in the spectral range from 50 kHz to 20 MHz. The frequency resolution is 156 Hz for a typical 0–1 MHz frequency scan, allowing for a high resolution of spectral features. A detailed schematic of the optical pathway for the LDV is given in [7].

The vibrometer measures the instantaneous velocity at a specific point on the MWNT. It is possible to integrate the velocity time series data to yield the displacement time series data, however this is not necessary since the focus of the present work is on measuring the resonance frequencies and Q-factors of the MWNT for which we need only examine the peaks in the frequency spectrum of velocity or displacement data. Another important practical reason for using the velocity spectrum to study resonance peaks is as follows: while the output of the LDV is proportional to the local velocity, the proportionality constant is known only when *most* of the reflected beam is collected by the sensor. When this condition is violated, for instance (a) when the laser spot lies on the edge of a vibrating structure or (b) as in our case when the vibrating object is much smaller than the spot size of the beam, then the measured signal is only proportional to the local velocity of the MWNT and a quantitative estimate of the local velocity or amplitude becomes problematic, even though the frequencies are accurately measured. Thus for the MWNT velocity or displacement spectra plotted in this paper we normalize the data (either displacement or velocity) to a maximum value of unity[4].

The MWNTs used in this experiment were grown at 900 °C in a SEKI AX5200S microwave PECVD reactor using Fe_2O_3 nanoparticle catalyst particles [10]. Individual MWNTs were affixed to etched nickel scanning tunneling microscopy (STM) tips using the procedure described by Stevens *et al* [11]. To make the MWNT attachment more robust, the Ni tip is first touched to soft double-sided carbon scanning electron microscope (SEM) tape (STR tape from Shinto Paint Co. Ltd). A small amount of adhesive from the SEM tape sticks to the Ni tip and helps affix the MWNT.

3. Results and discussion

3.1. Vibration spectra of bare MWNTs

After the vibration spectra from an individual MWNT were recorded, the length, L, and outer diameter, d_o, of the MWNT were measured using a Hitachi S-4800 field emission scanning electron microscope (FESEM). If L, d_o, and inner diameter, d_i, of a MWNT are known and if f_j of that MWNT can be accurately determined, then the elastic modulus, E, can be inferred from the well-known Euler–Bernoulli analysis of a clamped free oscillating cantilever. The undamped jth natural frequency of oscillation is given by

$$f_j = \frac{\alpha_j^2}{2\pi L^2}\sqrt{\frac{EI}{\rho A}} = \frac{\alpha_j^2}{8\pi L^2}\sqrt{\frac{E}{\rho}(d_o^2 + d_i^2)}, \tag{2}$$

where $\alpha_1 = 1.875$, $\alpha_2 = 4.694$, I, the areal moment, is $\pi(d_o^4 - d_i^4)/64$, ρ, the density of graphite, is (2300 kg m^{-3}), and A is the cross-sectional area of the MWNT, $\pi(d_o^2 - d_i^2)/4$. By accurately measuring f_j, equation (2) can be used to estimate the elastic modulus of the MWNT.

For each MWNT studied, 5–10 thermal vibration spectra were acquired and averaged to produce a resultant spectrum that was used for further analysis. One such spectrum taken from MWNT NT1 is shown in figure 1(b). For each MWNT, a background spectrum with the laser beam focused on the Ni tip is also acquired. The mass of the Ni tip is great enough that there should be no measurable thermal oscillations and indeed, measurements of a background spectra were uniformly featureless.

Vibration spectra from the MWNTs studied revealed peaks at both the first and second bending mode eigenfrequencies, f_1 and f_2. Table 1 summarizes the dimensions, resonant frequency peaks, and E for two bare MWNTs. We note the f_2/f_1 ratio for sample NT2 is 7.2, somewhat higher than the theoretical value of 6.3. However, the Euler–Bernoulli beam theory assumes straight, homogeneous beams while the MWNTs studied are curved, have carbonaceous deposits on the exterior, and, in some cases, exhibit non-uniform mass density along their length (see figure 1(c)). Any of these reasons might explain why the f_2/f_1 ratio does not exactly match the expected value of 6.3.

[3] This vibration isolation slab weights 30 000 kg, is supported by six air spring dampers, and meets NIST-A1 vibration standards.

[4] Technically, the velocity spectrum is determined directly from the Doppler shift. By contrast, the displacement spectrum is measured by counting the zero-crossing of the interference bands.

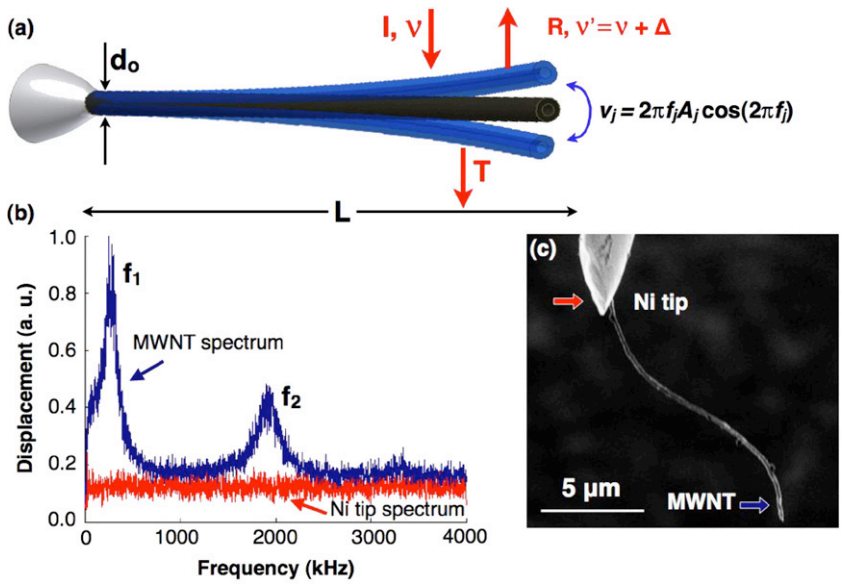

Figure 1. In (a), a schematic diagram of a MWNT affixed to a Ni STM tip. Typical dimensions for the MWNT are $d_o = 180$ nm and $L = 15$ μm. The reflected light (R) of the normally incident laser beam (I) is Doppler shifted by frequency Δ when reflected from the MWNT. In (b), the displacement frequency spectrum from MWNT NT1 shows eigenmode peaks at 230 and 1930 kHz attributed to the 1st and 2nd bending modes of the MWNT. In (c), an SEM micrograph shows the MWNT affixed to the Ni tip. The arrows represent where the laser vibrometer was focused on the bead and Ni tip.

Table 1. Experimentally measured modulus for the MWNTs studied. The calculations in this table assume $d_i = 0.5d_o$.[5] The estimated estimated errors are ± 10 nm for d_o, ± 0.2 μm for L, and ± 2 kHz for f_j.

Bare MWNT	d_o (nm)	L (μm)	f_1 (kHz)	f_2 (kHz)	E_1 (GPa)	E_2 (GPa)
NT1	230	14.4	285	1930	6.2 ± 0.8	7.3 ± 1.0
NT2	176	12.6	929	6730	66.0 ± 9.8	88.2 ± 13.2

3.2. Ultimate measurement limits

When a cylinder (such as a MWNT) is illuminated by light, the amount of light scattered and absorbed depends in a complicated way on the geometry and optical properties of the cylinder, the index of refraction of the surrounding medium, and the wavelength and polarization of the incident light beam (see figure 2(a)). When the incident wavelength becomes comparable to the dimensions of the cylinder, Mie scattering theory rather than geometrical optics is applicable. In Mie theory, the scattering cross section per unit length of the cylinder, C_{sca}, depends on the diameter of the cylinder d_o, the complex index of refraction of both the cylinder (N) and surrounding medium (N_{med}), and the wavelength (λ) and angle of incidence of the light beam. From these parameters, expressions for C_{sca} far from the cylinder can be derived [12]. A particularly useful quantity is the scattering efficiency Q_{sca}, which is defined as $Q_{sca} = C_{sca}/d_o$. If Q_{sca} is greater than 1, then light is effectively scattered from an apparent object that is larger in cross section than the actual scattering object.

[5] This assumption, $d_i = 0.5d_o$, is based on parallel studies of TEM micrographs of representative MWNTs.

We use Mie theory to calculate the scattering efficiency Q_{sca} of the MWNT, which is modeled as a dielectric cylinder of diameter d_o. This calculation allows us to better understand the limits of light scattering from a MWNT and to estimate the smallest diameter MWNT whose oscillation might be detected. A FORTRAN program for calculating Q_{sca} as a function of incident angle was modified to calculate Q_{sca} as function of d_o, N, and N_{med} [12]. Calculations of Q_{sca} are plotted in figure 2(b) and were performed for the case of circularly polarized 633 nm light, to match the conditions of our experiments.

Optical constants for MWNTs are not well established. However, a MWNT is similar in structure to pyrolytic graphite for which the optical constants are known. With this in mind, any light reflected from the front surface of a MWNT scatters from graphitic planes similar in orientation to the [0001] basal plane of graphite. Any light scattered from the outer edge of a MWNT reflects from graphitic planes similar in orientation to the $[11\bar{2}0]$ plane of graphite. Following this logic, realistic limits on Q_{sca} can be obtained using the appropriate optical constants of pyrolytic graphite [13].

We conclude from figure 2(b) that for diameters less than $\sim$250 nm, the edges of the MWNT will more effectively scatter light. Assuming that the signal-to-noise ratio (SNR) of the vibrational resonance peak is proportional to the amount of light scattered, we can estimate the smallest diameter MWNT that reflects just enough light so that its vibration might be detected. From our measured data, we typically find a SNR at resonance of 5:1. We define the smallest diameter MWNT whose vibration spectra can be measured as a MWNT that scatters light at resonance with a SNR of 1:1. From the calculations leading to figure 2(b), we estimate that MWNTs with diameters between 70 and 100 nm meet the SNR criterion

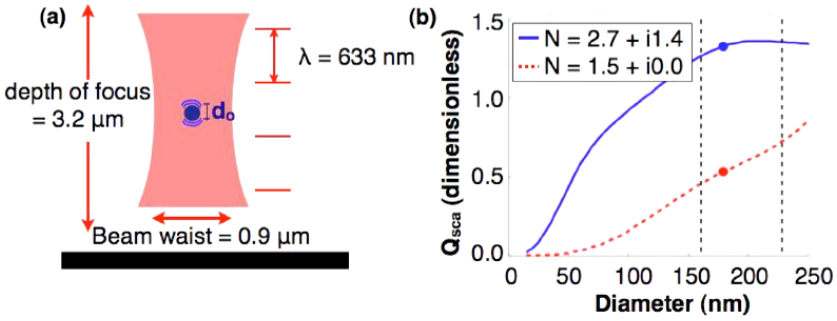

Figure 2. In (a), a schematic of the laser light focused on the MWNT with outer diameter d_o. As indicated by the shaded region, the 50× microscope objective focuses the beam to a waist much wider than the MWNT. In (b), the calculated Q_{sca} for circularly polarized 633 nm light normally incident on a graphitic cylinder in air as a function of diameter. The case of light scattering off the [0001] plane ($N = 1.5 + i0$; dotted red line) and the [11$\bar{2}$0] plane ($N = 2.7 + i1.4$; solid blue line) are considered. The diameters of MWNTs studied fall within the range indicated by the dashed vertical lines. The solid circles indicate the calculated Q_{sca} for a 180 nm diameter MWNT.

of 1:1. This suggests that MWNTs with diameters in the range between 70 and 100 nm are the smallest diameter MWNTs that can be studied using the Polytec MSA-400 scanning LDV.

Since Q_{sca} depends strongly on the index of refraction N of the cylinder, nanowires of materials other than carbon might scatter light more effectively, thereby allowing the vibrational spectra of smaller diameter nanowires to be detected. Consider the case of Si(111) nanowires which have $N = 3.9+i0.02$ [14]. Calculations give a Q_{sca} one to two orders of magnitude higher than MWNTs of the same diameter, suggesting that the oscillation of silicon nanowires can be measured to diameters substantially less than 100 nm.

3.3. Extension to smaller diameters: vibration spectra of MWNTs with beads

The lower diameter limit of 70–100 nm for detecting MWNT oscillations restricts this optical technique to relatively large diameter MWNTs. An additional complicating factor is that MWNTs and nanowires with a diameter of only 100 nm are not visible in the 50× bright-field optical microscope used to focus the laser light of the vibrometer. As a first step to measuring the vibration spectra of MWNTs and nanowires with smaller diameters, we developed a technique to add a small glass bead to the end of an individual MWNT. An advantage of adding a glass bead is the additional light that scatters from the bead makes the bead easier to align with the focused laser beam.

Partially gold-coated glass beads (Duke Scientific 9002 borosilicate glass spheres with diameter 2.0 ± 0.5 μm) were prepared and transferred to a MWNT using a 0.25 mm diameter Ni wire under the magnification of a 50× dark-field microscope. The Ni wire was first inserted into a vial containing the glass beads. Upon withdrawal, hundreds of glass beads were attached to the Ni wire. One side of each bead was then partially coated with a thin layer of gold after inserting the Ni wire into a thermal evaporator. An STM tip was then used to transfer an individual glass bead from the Ni wire to a MWNT by repeatedly pushing and pulling the MWNT against the bead.

In the case of a large mass added to the end of the MWNT ($m_{bead} \gg m_{MWNT}$), the mass of the MWNT can be neglected and the fundamental bending frequency f_{bend} can be approximated as $f_{bend} = \frac{1}{2\pi}\sqrt{k/m_{bead}}$. For a cantilevered beam $k = 3EI/L^3$, so the bending frequency is

$$f_{bend} = \frac{1}{2\pi}\sqrt{\frac{3EI}{L^3 m_{bead}}}. \quad (3)$$

Table 2. Experimentally measured elastic modulus for MWNTs with beads. The calculations in this table assume $d_i = 0.5d_o$. The estimated estimated errors are ±10 nm for d_o, ±0.2 μm for L, and ±2 kHz for f_j. Bead diameters (not listed, estimated error ±20 nm) were measured in the FESEM and used to estimate the mass of the bead.

MWNT with bead	d_o (nm)	L (μm)	m_{bead} (pg)	f_{bend} (kHz)	E (GPa)
NT3	160	14.0	12.1	44.9	29.3 ± 8.6
NT4	177	15.1	4.88	68.4	22.9 ± 6.0
NT5	176	14.7	17.1	53.3	60.8 ± 16.6

Thermal vibration spectra were recorded and averaged for several MWNTs with attached beads. Again, the background vibrational spectrum from the Ni tips was uniformly featureless. One such spectrum taken from MWNT NT5 is shown in figure 3(a). An electron micrograph of the MWNT with the gold-coated glass bead is given in figure 3(b). Table 2 summarizes the dimensions, resonance frequency peaks, and elastic modulus calculated for three MWNTs with glass beads affixed. The values of E are within the range of modulus values, $\bar{E}$ = 3–600 GPa, previously reported for CVD-grown MWNTs [15–18].

3.4. Quality factor

The quality factor, Q, of a specific eigenmode quantifies how much energy is dissipated during one oscillation cycle. High Q (small energy dissipation) is desirable for many applications. Reliable estimates for Q are often difficult to obtain since the measured shape of the resonance as a function of frequency is required for accurate Q determination.

A reliable approximation to the displacement spectrum of a cantilevered beam resonance is given by the magnitude of

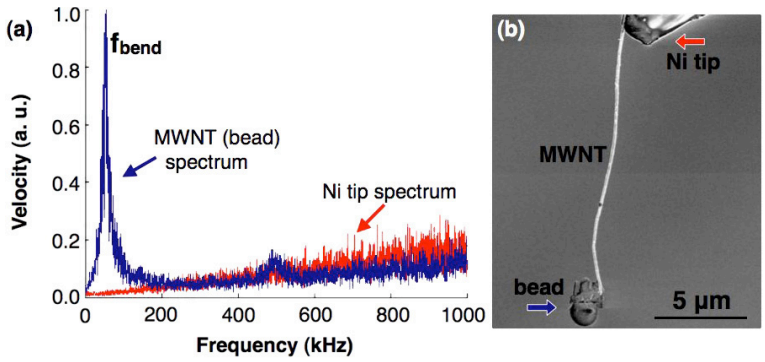

Figure 3. In (a), the velocity frequency spectrum of a MWNT showing a vibration peak at 53.3 kHz that is attributed to the bending oscillation of the MWNT. In (b), an SEM micrograph of the MWNT with a gold-coated glass bead affixed to the MWNT tip. The arrows represent where the laser vibrometer was focused on the bead and Ni tip.

Table 3. Quality factors for the MWNTs studied were determined by fitting equation (4) to the oscillation resonance spectrum.

Bare MWNT	f_1 (kHz)	Q_1	f_2 (kHz)	Q_2
NT1	285	2.8	1930	9.9
NT2	929	3.3	6730	18
MWNT with bead	f_{bend} (kHz)		Q	
NT3	44.9		5.9	
NT4	68.4		5.0	
NT5	53.3		6.2	

the frequency response function (equation (4)). By fitting the measured resonance to equation (4),

$$Z(\omega) = \frac{G}{\sqrt{\left[1-\left(\frac{\omega}{\omega_j}\right)^2\right]^2 + \left(\frac{\omega}{\omega_j Q}\right)^2}} + N, \tag{4}$$

the Q-factor of a given MWNT can be accurately determined. In equation (4), $Z(\omega)$ is the normalized amplitude of the MWNT oscillation, ω is the frequency at which $Z(\omega)$ was measured, G is the overall gain, ω_j is the resonant frequency ($\omega_j = 2\pi f_j$), and N is the noise offset. To fit the velocity spectrum, the displacement spectrum is differentiated with respect to time, which, in the frequency domain, amounts to multiplying the displacement spectrum by ω. After a least squares fit of the resonance data to equation (4) was performed, the Q-factor was calculated from the 3 dB points determined by the fit. The measured Q-factors for our spectra are reported in table 3. A notable feature of these Q values is they are considerably smaller when compared to micron-sized resonators. For example, Si microcantilevers commonly used in AFM applications typically have Q values of 100–500 when measured in air.

To understand why the measured Q values are small, we note that the measured Q-factor is given by an effective Q (Q_{eff}), where

$$\frac{1}{Q_{\text{eff}}} = \frac{1}{Q_{\text{gas}}} + \frac{1}{Q_{\text{clamp}}} + \frac{1}{Q_{\text{intrinsic}}}. \tag{5}$$

In equation (5), Q_{gas} accounts for the damping of the oscillating MWNT due to air, Q_{clamp} is the damping due to energy lost at the interface of the MWNT and Ni tip, and $Q_{\text{intrinsic}}$ represents the energy lost due to intrinsic defects in the MWNT itself.

The displacement of the MWNT at the Ni tip is several orders of magnitude smaller than the oscillation amplitude of the free end of the MWNT; thus we can treat the clamp as a rigid support, and therefore, $1/Q_{\text{clamp}}$ is negligible. From other experiments on MWNTs conducted in UHV, we estimate $Q_{\text{intrinsic}} \sim \text{O}(10^2)$ [3, 4]. We conclude that when a MWNT is vibrating in air, the majority of the energy is dissipated through gas damping.

To further check that gas damping is responsible for the small Q values, we calculate the Knudsen number, $Kn = \bar{\lambda}/d_{\text{o}}$, where $\bar{\lambda}$, the mean free path of air molecules, is 65 nm for air at STP. Thus the MWNTs we have studied have $Kn \approx 0.4$ indicating they are in a transition regime ($0.1 < Kn < 10$) [19] for which accurate gas damping models are not available. However at slightly greater Kn numbers ($Kn > 10$) the damping is in the free molecular regime and published theories can be used to estimate Q_{gas}.

In the free molecular regime, the primary source of damping is momentum transfer due to collisions with the surrounding gas molecules. Assuming a flexible beam and following Christian's model [20] for momentum transfer mediated gas damping in the free molecular regime, we find that an expression for gas damping of the jth eigenmode of the MWNT is given by

$$\left(Q_{\text{gas}}\right)_j = \frac{\omega_j \rho A}{4bP}\sqrt{\frac{\pi R_{\text{o}} T}{2M_{\text{m}}}}, \tag{6}$$

where P, R_{o}, and M_{m}, are the pressure, universal gas constant, and molar mass, respectively. In the case of a cylindrical beam, the effective area for damping per unit length, b, is $\pi d_{\text{o}}/4$ [21]. From equation (6), we calculate $(Q_{\text{gas}})_1$ to be on the order of unity for our MWNTs, which is comparable to the measured Q_{eff} listed in table 3. This further confirms that the small Q of MWNTs oscillating under ambient conditions arises naturally from gas damping.

Referring to table 3, we find that for the bare MWNTs, the Q of the second eigenmode is higher than the first. This result is due to the increased stiffness of the second eigenmode, since

the Q-factor is proportional to the square root of the modal stiffness [22]. Thus the increased Q is a direct consequence of the increased modal stiffness of the higher eigenmodes.

From table 3, we also observe that Q increases with the added mass of the beads. This increase in Q with added mass was recently reported for silicon cantilevers [23] and occurs because the Q factor is also proportional to the square root of the modal mass. When a bead is added the modal stiffness of the MWNT is unchanged, but its modal mass increases leading to an increase in Q.

4. Conclusions

Vibrating nanotubes and nanowires are gaining interest in a wide range of applications that range from sensing applications to nanoelectronics components. We have demonstrated the utility of a laser Doppler vibrometer (LDV) technique to measure the vibrational spectrum of a single nanotube. Scattering considerations based on Mie theory indicate that the LDV technique can provide useful data on MWNTs with diameters as small as 70–100 nm. Furthermore, we have also shown that for nanowires with diameters smaller than 70–100 nm, a gold-coated glass bead added near the free end of the nanowire can increase the reflectivity by a sufficient amount to allow a measurement of the nanowire's vibrational spectrum.

Using the laser vibrometer technique, the thermally excited vibration spectra of a number of PECVD-grown MWNTs were systematically measured. From the resonant frequencies, values for E for a set of five PECVD-grown MWNTs were obtained. The average E value measured in this study (40 GPa) is well within the range of E (3–600 GPa) previously reported for CVD-grown MWNTs.

The quality factors for the first mode of oscillation were found to be comparable to those reported for clamped–clamped MWNT devices in air ($Q = 3$–20) [5] and are in line with theoretical predictions of air damping in the free molecular gas damping regime. Models of gas damping predict Q values comparable to those measured experimentally, suggesting that gas damping is largely responsible for the broad resonance behavior observed under atmospheric conditions.

Acknowledgments

RT and AR are supported by Sandia National Laboratories under Contract No. 623235. LB is supported by a Purdue Excellence in Science and Engineering Fellowship from Sandia National Laboratories. P Amama and T Fisher are gratefully acknowledged for providing the MWNTs studied. J Melcher's insight into cantilever dynamics is greatly appreciated.

References

[1] Poncharal P, Wang Z L, Ugarte D and de Heer W A 1999 Electrostatic deflections and electromechanical resonances of carbon nanotubes *Science* **283** 1513–6

[2] Purcell S T, Vincent P, Journet C and Binh V T 2002 Tuning of nanotube mechanical resonances by electric field pulling *Phys. Rev. Lett.* **89** 276103

[3] Sazonova V, Yaish Y, Ustunel H, Roundy D, Arias T A and McEuen P L 2004 A tunable carbon nanotube electromechanical oscillator *Nature* **431** 284–7

[4] Witkamp B, Poot M and van der Zant H S J 2006 Bending-mode vibration of a suspended nanotube resonator *Nano Lett.* **6** 2904–8

[5] Garcia-Sanchez D, Paulo A S, Esplandiu M J, Perez-Murano F, Forro L, Aguasca A and Bachtold A 2007 Mechanical detection of carbon nanotube resonator vibrations *Phys. Rev. Lett.* **99** 085501

[6] Conley W, Raman A, Krousgrill C and Mohammadi S 2008 Nonlinear and nonplanar dynamics of suspended nanotube and nanowire resonators *Nano Lett.* **8** 1590–5

[7] Portoles J F, Cumpson P J, Hedley J, Allen S, Williams P M and Tendler S J B 2006 Accurate velocity measurements of AFM-cantilever vibrations by Doppler interferometry *J. Exp. Nanosci.* **1** 51–62

[8] Ricci J and Cetinkaya C 2007 Air-coupled acoustic method for testing and evaluation of microscale structures *Rev. Sci. Instrum.* **78** 055105

[9] Belov M, Quitoriano N J, Sharma S, Hiebert W K, Kamins T I and Evoy S 2008 Mechanical resonance of clamped silicon nanowires measured by optical interferometry *J. Appl. Phys.* **103** 074304

[10] Amama P B, Cola B A, Sands T D, Xu X F and Fisher T S 2007 Dendrimer-assisted controlled growth of carbon nanotubes for enhanced thermal interface conductance *Nanotechnology* **18** 385303

[11] Stevens R, Nguyen C, Cassell A, Delzeit L, Meyyappan M and Han J 2000 Improved fabrication approach for carbon nanotube probe devices *Appl. Phys. Lett.* **77** 3453–5

[12] Bohren C F and Huffman D R 1983 *Absorption and Scattering of Light by Small Particles* (New York: Wiley)

[13] Greenaway D L, Harbeke G, Bassani F and Tosatti E 1969 Anisotropy of optical constants and band structure of graphite *Phys. Rev.* **178** 1340–8

[14] Aspnes D E and Studna A A 1983 Dielectric functions and optical parameters of Si, Ge, GaP, GaAs, GaSb, InP, InAs, and InSb from 1.5 to 6.0 eV *Phys. Rev.* B **27** 985–1009

[15] Salvetat J P, Kulik A J, Bonard J M, Briggs G A D, Stockli T, Metenier K, Bonnamy S, Beguin F, Burnham N A and Forro L 1999 Elastic modulus of ordered and disordered multiwalled carbon nanotubes *Adv. Mater.* **11** 161–5

[16] Gaillard J, Skove M and Rao A M 2005 Mechanical properties of chemical vapor deposition-grown multiwalled carbon nanotubes *Appl. Phys. Lett.* **86** 233109

[17] Guhados G, Wan W K, Sun X L and Hutter J L 2007 Simultaneous measurement of Young's and shear moduli of multiwalled carbon nanotubes using atomic force microscopy *J. Appl. Phys.* **101** 033514

[18] Lee K M, Lukic B, Magrez A, Seo J W, Briggs G A D, Kulik A J and Forro L 2007 Diameter-dependent elastic modulus supports the metastable-catalyst growth of carbon nanotubes *Nano Lett.* **7** 1598–602

[19] Bhiladvala R B and Wang Z J 2004 Effect of fluids on the Q factor and resonance frequency of oscillating micrometer and nanometer scale beams *Phys. Rev.* E **69** 036307

[20] Christian R G 1966 Theory of oscillating-vane vacuum gauges *Vacuum* **16** 175–8

[21] Newell W E 1968 Miniaturization of tuning forks *Science* **161** 1320–6

[22] Melcher J, Hu S Q and Raman A 2007 Equivalent point-mass models of continuous atomic force microscope probes *Appl. Phys. Lett.* **91** 053101

[23] Dhayal B, Post N, Melcher J, Raman A, Chiu G and Reifenberger R 2008 Enhancing microcantilever quality factor by controlling mass distribution, in preparation